Boletim da Sociedade Astronômica Brasileira, **37**, no. 1, 157-159

RE J0317 – 853 as a product of a white dwarf merger

A study of rotational evolution

I. A. Lacerda[1], M. F. Sousa[2] & J. G. Coelho[1]

[1] Universidade Federal do Espírito Santo, Vitória, ES
e-mail: isabelle.lacerda@edu.ufes.br, jaziel.coelho@ufes.br
[2] Universidade de São Paulo, São Carlos, SP
e-mail: mfelipe.sousa@ifsc.usp.br

Abstract. Massive, magnetic, and rapidly rotating white dwarfs challenge single-star evolutionary models, suggesting an origin in double white dwarf mergers. These objects exhibit masses near the Chandrasekhar limit, magnetic fields of 10^6–10^9 G, and spin periods of minutes to seconds. We present a theoretical analysis of the massive (1.35 $M_\odot$), highly magnetic (B = 450 MG), and rapidly rotating (P = 725.7 s) white dwarf RE J0317 − 853, proposing it as a post-merger remnant. Using a rotational evolution model, we derive an accretion rate of 1.13×10^{-7} $M_\odot$ yr^{-1} and predict a spin-down rate of 8.14×10^{-16} s s^{-1}, consistent with an estimated cooling age of 0.2 Gyr. These results support the merger hypothesis and motivate future observations to measure rotational braking.

Resumo. Anãs brancas massivas, magnéticas e de alta rotação desafiam o modelo de evolução de uma estrela isolada, sugerindo uma origem na coalescência de binárias de anãs brancas. Esses objetos apresentam massas próximas ao limite de Chandrasekhar, campos magnéticos entre 10^6 e 10^9 G e períodos de rotação da ordem de minutos a segundos. Apresentamos uma análise teórica da anã branca massiva (1.35 $M_\odot$), altamente magnética (B = 450 MG) e de rápida rotação (P = 725.7 s), RE J0317 − 853, propondo que seja a remanescente de uma fusão de anãs brancas. Utilizando um modelo de evolução rotacional, calculamos uma taxa de acreção de 1.13×10^{-7} $M_\odot$ ano^{-1} e uma taxa de desaceleração 8.14×10^{-16} s s^{-1}, consistentes com a idade de resfriamento estimada em 0.2 Ga. Esses resultados apoiam a hipótese de origem por fusão e motivam futuras observações para a medição da desaceleração rotacional.

Keywords. Stars: evolution – Stars: white dwarfs

1. Introduction

The population of white dwarfs includes isolated sources and binary systems with a range of peculiar properties. A notable subset displays unusual characteristics such as being massive, highly magnetic, and rapidly rotating. These features are difficult to reproduce within a single-star evolutionary framework, leading to the hypothesis that they are remnants of double white dwarf mergers (Barstow et al. 1995; Ferrario et al. 1997; Vennes et al. 2003).

The coalescence of white dwarf binaries also represents a potential trigger for Type Ia supernovae and, in the case of the gravitational collapse of an unstable remnant, a formation channel for neutron stars (Maoz, Mannucci & Nelemans 2014; Shen 2015; Schwab 2021). Anomalous X-ray pulsars and soft gamma-ray repeaters may be associated with high mass, short rotation period, strongly magnetized white dwarf remnants (Coelho & Malheiro 2014).

Numerical simulations employing smoothed particle hydrodynamics support the hypothesis that white dwarf mergers can produce massive remnants with strong magnetic fields (Guerrero et al. 2004; Yoon et al. 2007; Lorén-Aguilar et al. 2009; García-Berro et al. 2012). In the simulations, when the merger occurs, most of the primary star's material forms the central white dwarf remnant. Half of the secondary's mass is redistributed into a hot spherical envelope around it, while the remaining material forms a self-gravitating Keplerian disk. Additionally, a small amount of matter ($\approx 10^{-3}$ $M_\odot$) is ejected.

Our object of study is the extreme ultraviolet source RE J0317 − 853 (also identified as EUVE J0317-85.5). This white dwarf belongs to a class of objects thought to originate from an evolutionary channel different from that of single-star evolution, standing out due to its extreme properties: a mass near the Chandrasekhar limit ($\log g$ = 9.5, corresponding to 1.35 $M_\odot$), a spin period of 725.7 s (Vennes et al. 2003), and a dipolar magnetic field of 450 MG (Barstow et al. 1995; Ferrario et al. 1997). Additional evidence for a non-standard origin arises from its association with the non-magnetic white dwarf companion LB 9802, whose estimated cooling age is inconsistent with expectations from single-star evolution for their respective masses. The former and more massive object has an estimated cooling age of 0.1 – 0.3 Gyr, while its companion, with $\log g = 8.19 \pm 0.05$ (Barstow et al. 1995), has a cooling age of about 0.4 Gyr (Ferrario et al. 1997).

This work investigates whether the merger of double white dwarf systems can result in a stable, rapidly rotating, massive, and strongly magnetic white dwarf. To do so, we employ the modeling approach introduced by Sousa et al. (2022), which was used to study the rotational evolution of SDSS 221141.80 + 113604.4 and ZTF J190132.9 + 145808.7. By incorporating observational constraints and estimates for the physical properties of RE J0317 − 853, we aim to evaluate the rotational evolution of its merger remnant and examine whether the model can reproduce the observed rotation period given an estimated cooling age.

2. Rotational Evolution of the Post-merger Remnant

Numerical smoothed-particle hydrodynamics simulations demonstrate that double white dwarf mergers can produce massive remnants with strong magnetic fields (Guerrero et al. 2004; Yoon et al. 2007; Lorén-Aguilar et al. 2009; García-Berro et al. 2012). In this scenario, most of the primary mass forms the central remnant, while material from the secondary settles into a hot envelope and a rapidly rotating Keplerian disk, and only $\sim 10^{-3}\ M_\odot$ is ejected.

After disk formation, the remnant interacts with the disk, driving accretion or matter ejection and modifying its angular momentum through associated torques (Becerra et al. 2018). The mass flow is regulated by the fastness parameter ω as defined in Eq. 1]. The values $\omega < 1$ correspond to the accretion regime, while $\omega > 1$ lead to the *propeller* regime, associated with matter ejection.

$$\omega = \frac{\Omega}{\sqrt{GM/r_i^3}} \quad (1)$$

The evolution of angular momentum is given by Eq. 2, which combines the dynamic torque (T_{acc}) and the magnetic torque (T_{mag}), with I denoting the moment of inertia.

$$T_{\rm tot} = T_{\rm acc} + T_{\rm mag} \approx I\dot{\Omega} \quad (2)$$

Eqs. 3 and 4 describe, respectively, the torque generated by accretion or *propeller* action and the torque arising from magnetic effects. The radius R_m is the Alfvén (magnetospheric) radius, as discussed in Sousa et al. (2022) and originally in Pringle & Rees (1972). Magnetic torque, arising from dipole radiation and disk–field coupling, initially included both dipolar and quadrupolar components. However, as shown by Sousa et al. (2022), the quadrupolar component becomes negligible at low angular velocities, where the dipole term is much more significant. We therefore omit the quadrupolar contribution in our final model.

$$T_{acc} = \dot{M}\sqrt{GMR_m}\,(1-\omega) \quad (3)$$

$$T_{mag} = -\frac{2}{3}\frac{B^2R^6\Omega^3}{c^3}\sin^2\alpha \quad (4)$$

The rotational evolution proceeds through three stages. In *Phase I*, dynamic torques dominate, producing rapid spin-up or spin-down. *Phase II* occurs near equilibrium ($\omega \approx 1$) as the disk is depleted. Once the disk is exhausted, *Phase III* is driven solely by magnetic braking.

The duration of each phase follows from the angular momentum equation with the appropriate torque terms. *Phase I* can be solved considering $T_{tot} \approx T_{acc}$, while *Phase II* is set by the disk depletion timescale. During *Phase III* magnetic torque alone determines the time needed to reach the observed period. This framework yields an expression for the accretion rate ($\dot{M}$) and identifies the parameter range for which the rotational evolution is consistent with the observational constraints. Eq. 5 provides the accretion rate expressed in terms of observational parameters.

$$\dot{M} = \frac{B^2R^6\Omega_{obs}^{7/3}}{\sqrt{2}(GM)^{5/3}}\left(1 - \frac{2k_{dip}\Omega_{obs}^2}{I}\Delta t_{obs}\right)^{-7/6}, \quad (5)$$

where k_{dip} is described by:

$$k_{dip} = \frac{2}{3}\frac{B^2R^6}{c^3}\sin^2\alpha \quad (6)$$

3. Discussion and Conclusions

In our analysis, we adopt a mass of $1.35\,M_\odot$ and a dipolar magnetic field strength of 450 MG for RE J0317 − 853, following Ferrario et al. (1997). We consider the spin period of 725.7 s (Vennes et al. 2003) as the final rotational period, corresponding to a rotational age of 0.2 Gyr, consistent with the estimated cooling age range (Ferrario et al. 1997).

As initial conditions, we explore two values for the initial spin period, one below and another above the equilibrium period ($P_{eq} = 2\pi/\Omega_{eq} = 720.5$ s). Figure 1 shows the rotational evolution for these parameters, demonstrating that the equilibrium period is reached on the same timescale regardless of the initial value.

We compute an accretion rate of $\dot{M} = 1.13 \times 10^{-7} M_\odot\ {\rm yr}^{-1}$, compatible with the adopted parameters. Our model reproduces the observed period within 1.99×10^8 years of evolution, consistent with the cooling age. In this framework, the rotational evolution of RE J0317–853 supports a white dwarf merger origin. We also estimate a spin-down rate due to magnetic braking of $\dot{P} = 8.14 \times 10^{-16}$ s s^{-1}. A future observational determination of $\dot{P}$ for this white dwarf would provide an important test of this scenario.

Although the coalescence of double white dwarfs has not yet been observed in real time, newly operational facilities such as the Vera Rubin Observatory are expected to detect hundreds of merger-related optical transients annually (Sousa et al. 2023). Such observations will provide a unique opportunity to study merger remnants and to directly test the predictions of our model.

Acknowledgements. I. A. L. is grateful for the support provided by CAPES during the development of this research, as well as the funding from FAPES that has allowed us to continue our work in this area. The author also thanks PPGCosmo (UFES) for the support that allowed them to attend the XLVIII Reunião Anual da S.A.B.. M.F.S. thanks a Fundação de Amparo à Pesquisa do Estado de São Paulo (FAPESP, grants No. 2025/05794-2 and No. 2021/01089-1) for the financial support. J.G.C. is grateful for the support of FAPES (1020/2022, 1081/2022, 976/2022, 332/2023), CNPq (311758/2021-5, 306018/2025-0), and FAPESP (grant No. 2021/01089-1).

References

Barstow M. A., Jordan S., O'Donoghue D., Burleigh M. R., Napiwotzki R., Harrop-Allin M. K., 1995, MNRAS, 277, 971.
Becerra L., Rueda J. A., Lorén-Aguilar P., García-Berro E., 2018, ApJ, 857, 134.
Coelho G., Malheiro M., 2014, PASJ, 66, 14.
Ferrario L., Vennes S., Wickramasinghe D. T., Bailey J. A., Christian D. J., 1997, MNRAS, 292, 205.
García-Berro E., Lorén-Aguilar P., Aznar-Siguán G., Torres S., Camacho J., Althaus L. G., Córsico A. H., Külebi B., Isern J., 2012, ApJ, 749, 25.
Guerrero J., García–Berro E., Isern J., 2004, A&A, 413, 257.
Lorén-Aguilar P., Isern J., García-Berro E., 2009, A&A, 500, 1193.
Maoz D., Mannucci F., Nelemans G., 2014, *Annual Review of Astronomy and Astrophysics*, 52, 107.
Pringle J. E., Rees M. J., 1972, A&A, 21, 1.
Schwab J., 2021, ApJ, 906, 53.
Shen K. J., 2015, ApJ, 805, L6.
Sousa, M. F., Coelho, J. G., de Araujo, J. C. N., Kepler, S. O., & Rueda, J. A. 2022, ApJ, 941, 28.
Sousa, M. F., Coelho, J. G., de Araujo, J. C. N., Guidorzi, C., & Rueda, J. A. 2023, ApJ, 958, 134.
Vennes S., Schmidt G. D., Ferrario L., Christian D. J., Wickramasinghe D. T., & Kawka A., 2003, ApJ, 593, 1040.
Yoon S.-C., Podsiadlowski P., Rosswog S., 2007, MNRAS, 380, 933.

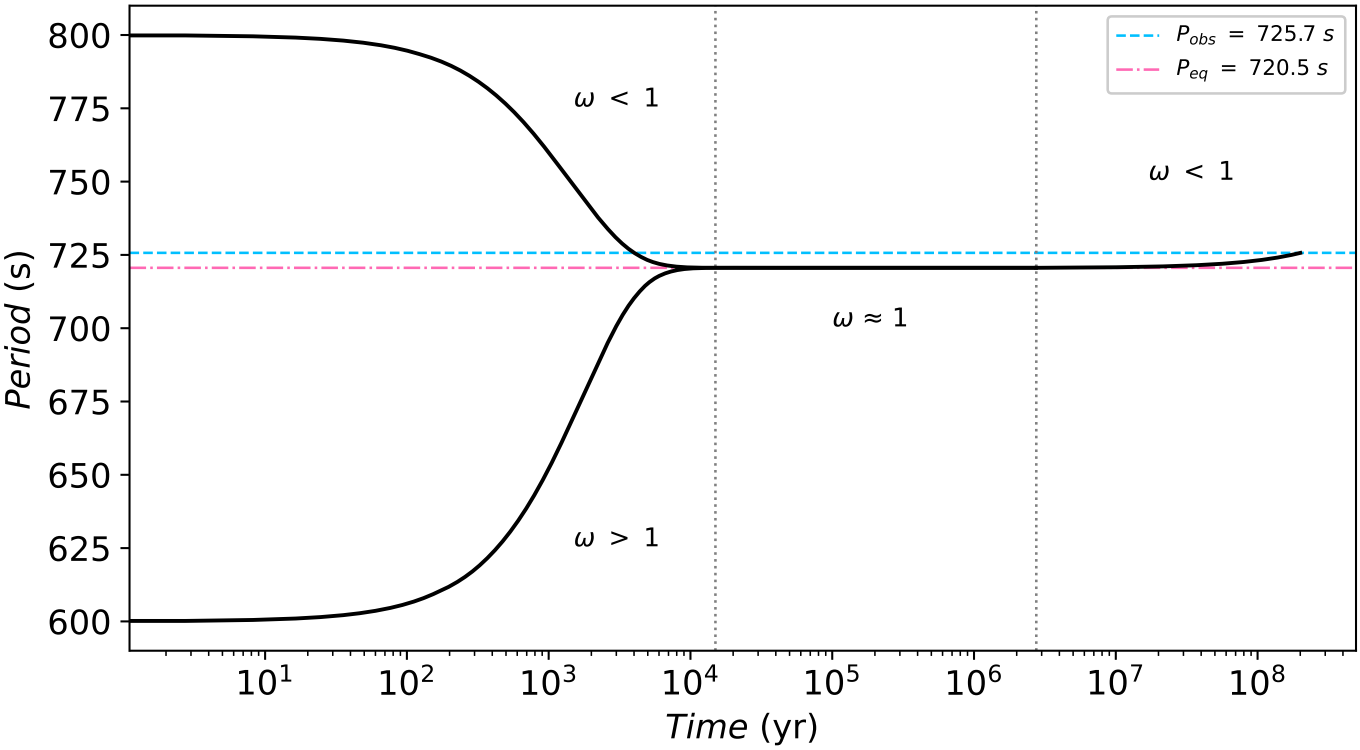

Figure 1. Evolution of the rotation period of RE J0317-853 (EUVE J0317-85.5) for an accretion rate of $\dot{M} = 1.13 \times 10^{-7}$ $M_\odot$/year and for different initial rotation periods, $P_0 = (600, 800)$ s. The dashed blue line indicates the observed period $P_{obs} = 725.7$ s, while the pink line represents the estimated equilibrium period $P_{eq} = 720.5$ s. The vertical dashed lines divide the evolutionary process into three phases according to the fastness parameter ω. The first phase can begin with $\omega < 1$ or $\omega > 1$, depending on whether the initial period is above or below the equilibrium period, respectively.